ARCHIVES OF ACOUSTICS
6, 2, 89-110 (1981)

A MODEL OF PISTON IMPACT AND VIBRATION FOR INTERNAL COMBUSTION ENGINE NOISE REDUCTION

A. F. SEYBERT

Department of Mechanical Engineering, University of Kentucky
(Lexington, Kentucky 40506, USA)

J. F. HAMILTON, P. A. HAYES

Department of Mechanical Engineering, Purdue University
(W. Lafayette, Indiana 47907, USA)

In this paper a mathematical model is developed to study piston impact and cylinder liner vibration in internal combustion engines. The aim of this study is to assess the effect on cylinder liner response (and, therefore on piston-impact induced noise) of certain design modifications such as cylinder liner stiffness, piston mass, and piston/cylinder liner running clearance. A single-mode representation of cylinder liner vibration is developed using the assumed modes method, where the cylinder liner is modeled as a thin cylindrical shell with fixed-free boundary conditions. Expressions for the kinetic and potential energy of the system, and for the generalized mass and stiffness of the system are developed. Lagrange's equation of motion is used to derive a differential equation of cylinder liner motion. The equation of motion for the piston is derived by assuming that the piston motion is pure translation. The initial conditions for cylinder liner response are developed from the conservation of momentum of the piston and the cylinder liner at impact. Experimental cylinder liner vibration data from a diesel engine are used to verify the accuracy of the piston impact model. Agreement between the experimental data and the cylinder liner response predicted by the mathematical model is generally good, but some discrepancies do exist. A computer simulation of the model is used to study the effect of parameter changes.

List of symbols

a' – radius of cylinder liner
A – area of the top surface of the piston

E — elastic modulus of cylinder liner material
F — horizontal force applied to the piston
h' — thickness of cylinder liner
k_{11} — generalized stiffness of the cylinder liner
L — length of cylinder liner
m_{11} — generalized mass of the cylinder liner
M — mass of the piston
M_p — generalized mass of the piston
n — circumferential mode number
P — cylinder pressure
q_i — generalized coordinates of the cylinder liner
Q — generalized force on the cylinder liner
R — distance from crankshaft axis to the top of the cylinder liner
R_1 — radius of crankshaft
R_2 — length of connecting rod
t — time
T — kinetic energy
V — potential energy
x — longitudinal coordinate of the cylinder liner
x_1 — longitudinal position of piston pin
y — normal displacement of the cylinder liner
α — angular coordinate of the cylinder liner
ζ — damping ratio
η — displacement of the piston
θ — angular rotation of the crankshaft
μ — Poisson's ratio for cylinder liner material
ϱ — density of cylinder liner material
Φ_i — normalized mode shapes of cylinder liner
Φ_x — mode shape of cylinder liner in the x direction
Φ — mode shape of cylinder liner in the α direction
ω_a — angular velocity of the crankshaft
ω_n — natural frequency of cylindrical shell

1. Introduction

Vehicle noise, particularly noise from trucks and buses, is a major source of annoyance to people living in industrialized urban areas in this country, as well as England, Japan, and most industrialized European countries. The United States and several other countries regulate the amount of noise emitted by heavy trucks and other types of vehicles. In the United States, for example, the Environmental Protection Agency [1] has established noise limit regulations for new medium and heavy trucks stating that the noise level shall not exceed 83 dB(A) (measured at 15.2 m from the side of the truck during a pass-by test) beginning in January 1978. Another set of regulations [2] applies to users of medium and heavy trucks.

Most heavy trucks are powered by diesel engines. Because of increased power requirements and energy considerations, the percentage of medium trucks using diesel engines is increasing. Diesel engines are noisier than spark ignition engines of similar horsepower rating because of a high peak cylinder pressure and a short cylinder pressure rise-time during ignition.

Extensive studies have been conducted to define the sources of noise of diesel engines [3]. Combustion excitation is the main source of noise for naturally-aspirated engines, while piston impact and other mechanical noise sources are of secondary importance. However, for turbo-charged engines, piston-impact generated noise is more important than combustion and other mechanical noise sources [4]. In a turbo-charged diesel engine the peak cylinder pressure, and, therefore, the forces that accelerate the piston, is higher than the peak cylinder pressure in a naturally-aspirated diesel engine. On the whole, however, turbo-charged diesel engines are quieter than their naturally-aspirated counterparts because turbo-charging smooths the combustion process, thereby reducing the combustion noise.

Fig. 1 shows two one-third octave spectra of the noise of a 350 hp turbo-charged diesel engine commonly used in heavy trucks. The upper spectrum is the noise of the engine fitted with standard pistons; the lower spectrum is the

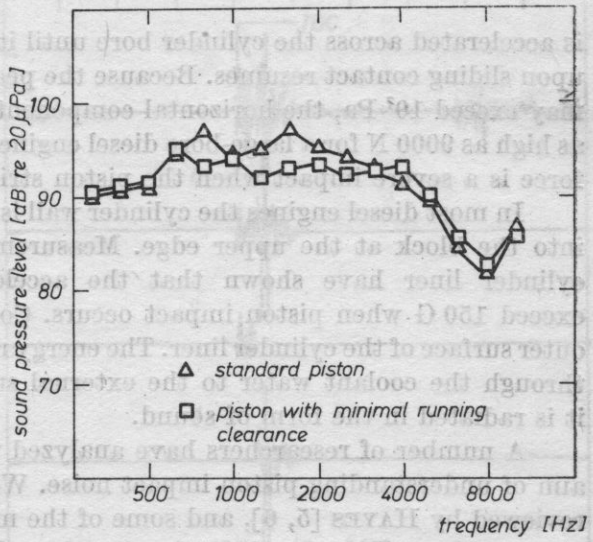

Fig. 1. Diesel engine noise spectra showing the importance of piston impact

noise of the same engine fitted with oversize pistons to minimize piston impact. A reduction of the overall noise by about 3-4 dB(A) was observed by this modification, indicating that piston impact accounts for at least fifty percent of the sound power of this engine.

The mechanisms of the piston impact phenomenon can be seen in simplified fashion in Fig. 2. During the compression phase of an engine cycle the piston is held in sliding contact with one side of the cylinder bore by the horizontal component of the force applied to the piston pin by the connecting rod. This force component reverses direction at top-dead-center (TDC); and the piston

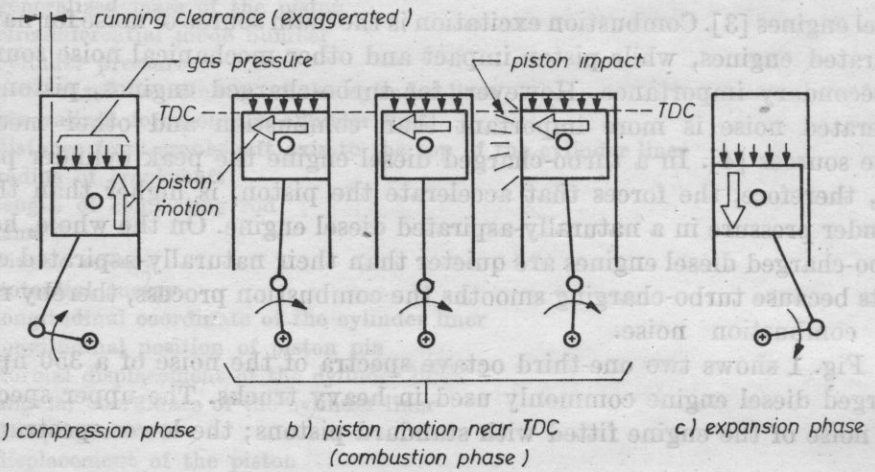

Fig. 2. Sequence of events showing piston-impact phenomenon

is accelerated across the cylinder bore until it impacts the opposite side, whereupon sliding contact resumes. Because the peak pressure in the cylinder at TDC may exceed 10^7 Pa, the horizontal component of the force on the piston can be as high as 9000 N for a large-bore diesel engine. The result of this large horizontal force is a severe impact when the piston strikes the cylinder wall.

In most diesel engines the cylinder wall is actually a cylindrical shell pressed into the block at the upper edge. Measurements on the outer surface of the cylinder liner have shown that the acceleration of the cylinder liner can exceed 150 G when piston impact occurs. Coolant water circulates around the outer surface of the cylinder liner. The energy released upon impact is transmitted through the coolant water to the external surfaces of the engine block where it is radiated in the form of sound.

A number of researchers have analyzed the motion of the piston with the aim of understanding piston impact noise. Work in this field has recently been reviewed by HAYES [5, 6], and some of the more comprehensive studies will be discussed here. FIELDING [7, 8] developed an elaborate set of equations describing the behavior of the piston as it travels across the cylinder bore. He used the final velocity of the piston to calculate the impact energy (kinetic energy on impact) of the piston on the cylinder liner. This parameter was used to estimate what effect certain design changes would have on piston-impact induced noise. FUJIMOTO, et al., [9-11] have studied the effect of oil-film cushioning and ring-groove

friction on piston motion. They used a reciprocating compressor to avoid the complications of combustion, and obtained some photographs showing piston contact area by using a transparent cylinder liner.

Neither of the above studies considered the behavior of the cylinder liner after impact. HADDAD and FORTESCUE [12] and HADDAD [13] have used an analog computer simulation to study the vibration of the cylinder liner. They used a two-mode expansion to represent the cylinder liner.

The remainder of this paper discusses a mathematical model for piston impact and cylinder liner vibration. Of particular importance in this study was the response of the cylinder liner to piston impact. Another aspect of this study [6] was concerned with developing a coherence model to predict piston impact noise. The cylinder liner vibration is used as an input parameter in the model.

2. Experimental observations

As a preliminary to the mathematical model, several experiments were conducted to determine the characteristics of piston impact and vibration. Accelerometers were mounted inside the coolant passage on the external surface

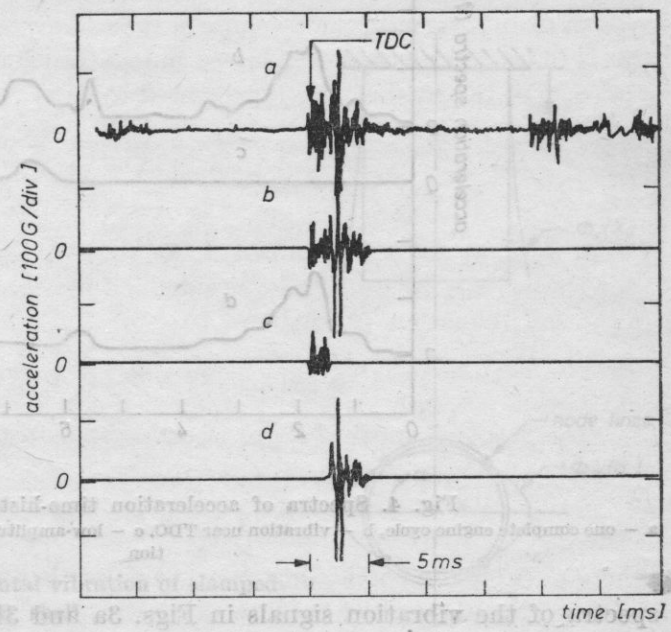

Fig. 3. Typical cylinder liner acceleration time-histories
a – one complete engine cycle (720° of crankshaft rotation), b – major vibration near TDC, c – low-amplitude vibration, d – high amplitude vibration due to piston impact

of the cylinder liners of the diesel engine described with reference to Fig. 1. These accelerometers were mounted at a point on the cylinder liners corresponding to the midpoint of the piston at impact. Fig. 3 shows a typical acceleration

time history, for approximately 720° of crankshaft rotation, with the engine operating at rated horsepower. As can be seen from Fig. 3a, the most significant region of vibration (typically 125 G maximum acceleration) begins slightly prior to TDC (between the compression and expansion strokes) and has a duration of about 5 ms. Figure 3a also reveals vibration due to five other lesser piston impacts that may occur during the intake, compression, expansion, and exhaust cycles of the engine, as well as vibration due to other mechanical forces. The piston impact near TDC is almost always the most important of the six piston impacts that may occur for each 720° of crankshaft rotation [11, 12]. All the vibration except the major vibration near TDC was edited from the data, Fig. 3b. The effect of this can be seen in Figs. 4a and 4b which show the

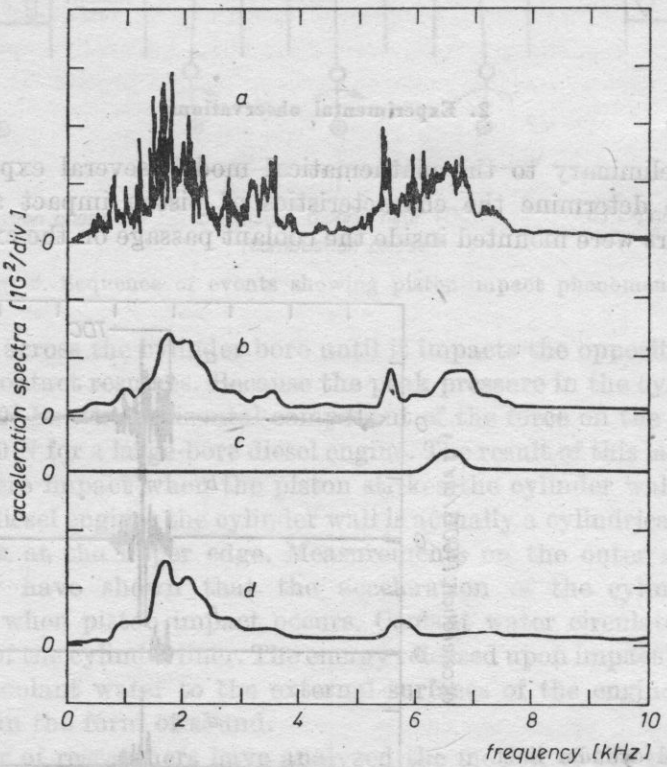

Fig. 4. Spectra of acceleration time-histories in Fig. 3
a – one complete engine cycle, b – vibration near TDC, c – low-amplitude vibration, d – high-amplitude vibration

spectra of the vibration signals in Figs. 3a and 3b, respectively. This editing procedure was used to make interpretation of the spectra easier, as seen by comparing Figs. 4a and 4b. There was not a sufficient number of data cycles available to smooth the spectrum in Fig. 4a using traditional ensemble-averaging techniques. The vibration time-history was further edited when it was noticed

that the vibration near TDC consisted of two parts: a low-amplitude vibration beginning just prior to TDC and lasting about 2 ms, followed by a high-amplitude vibration lasting approximately 3 ms. It was observed that the low-amplitude vibration was very high frequency and random in nature, and it did not repeat well from engine cycle to cycle. On the other hand, the high-amplitude vibration (due to piston impact) was quite repeatable from cycle to cycle. The spectra of the vibration time histories in Figs. 3c and 3d are shown in Figs. 4c and 4d, respectively.

From Figs. 3 and 4 it can be seen that piston impact causes the cylinder liner to vibrate over a broad range of frequencies between 1000 and 3000 Hz, with a maximum vibration around 1900 Hz. The data in Fig. 1 seem to support this conclusion as well. The natural frequencies ω_n of a circular cylinder of uniform thickness, clamped at one end and free at the other, are given by [14]:

$$\omega_n = \frac{1}{a'}\sqrt{\left(\frac{0.595\pi}{n}\right)^4\left(\frac{a'}{L}\right)+\frac{n^4}{12(1-\mu^2)}\left(\frac{h'}{a'}\right)^2}\sqrt{\frac{E}{\varrho}}, \qquad (1)$$

where a', h' and L are the shell radius, thickness, and length, respectively, and where E, ϱ, and μ are the Young's modulus, density, and Poisson's ratio, respectively, of the shell material. The natural frequencies given by equation (1) are for modes with no circumferential node lines and $2n$ longitudinal node lines.

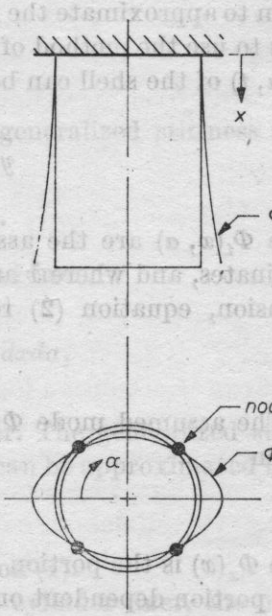

Fig. 5. Mode shape for fundamental vibration of clamped-free cylindrical shell

The lowest natural frequency for such a shell is when $n = 2$ [14], i.e., the shell cross-section deforms into the shape of an ellipse, see Fig. 5. For the steel cylinder liner in the diesel engine used in this study: $L = 277$ mm, $a' = 74.7$ mm, and

$h' = 8.26$ mm which yields a natural frequency of 1600 Hz using equation (1). In reality, the cylinder liner is restrained slightly at the lower end by a viscoelastic gasket. This would cause the actual natural frequency to be somewhat higher than equation (1) predicts.

Mechanical impedance tests were carried out to measure the natural frequency and mode shape of the cylinder liner. This was accomplished by removing the piston from one of the cylinders and attaching a small vibration exciter at the point on the cylinder liner where piston impact occurs. This test revealed the existence of the elliptical mode at approximately 1800 Hz.

The preliminary tests described above indicated that the cylinder liner was responding to piston impacts at its fundamental resonant frequency, and that higher modes were not important. Note, however, that Fig. 4 shows some vibration response near 6 kHz that may be the result of higher modes. But, from the practical viewpoint of noise reduction, only noise in the 500-3500 Hz region is important (see Fig. 1).

3. Piston impact model

When a single vibration mode dominates the overall response of a complex dynamic system, it is convenient to define an equivalent single-degree-of-freedom system to approximate the response of the real system. One way of accomplishing this is to use the method of assumed modes. In general, the normal displacement $y(x, a, t)$ of the shell can be represented by [15]

$$y(x, a, t) = \sum_{i=1}^{m} \Phi_i(x, a) q_i(t), \tag{2}$$

where $\Phi_i(x, a)$ are the assumed mode shapes, where $q_i(t)$ are the generalized coordinates, and where x and a are defined in Fig. 5. For a single mode ($m = 1$) expansion, equation (2) reduces to:

$$y(x, a, t) = \Phi_1(x, a) q_1(t). \tag{3}$$

The assumed mode $\Phi(x, a)$ is orthogonal in terms of x and a and can be written

$$\Phi_1(x, a) = \Phi_x(x) \Phi_a(a), \tag{4}$$

where $\Phi_x(x)$ is the portion of the assumed mode dependent only on x and $\Phi_a(a)$ is the portion dependent only on a (see Fig. 5).

The assumed mode shape was chosen such that the deflection $\Phi_x(x)$ along the length of the cylinder was the static deflection due to a uniformly distributed force. The deflection $\Phi_a(a)$ along the cylinder circumference was chosen to have four node lines.

Thus:

$$\Phi_x(x) = 2\left(\frac{x}{L}\right)^2 - \frac{4}{3}\left(\frac{x}{L}\right)^3 + \frac{1}{3}\left(\frac{x}{L}\right)^4, \qquad \Phi_\alpha(\alpha) = \cos 2\alpha,$$

and

$$\Phi_1(x, \alpha) = \left\{2\left(\frac{x}{L}\right)^2 - \frac{4}{3}\left(\frac{x}{L}\right)^3 + \frac{1}{3}\left(\frac{x}{L}\right)^4\right\}\cos 2\alpha. \tag{5}$$

Regarding external forces as nonconservative, Lagrange's equation of motion has the form

$$\frac{d}{dt}\left(\frac{\partial T}{\partial \dot{q}_1}\right) - \frac{\partial T}{\partial q_1} + \frac{\partial V}{\partial q_1} = Q(t), \tag{6}$$

where $Q(t)$ is the generalized force, and where T and V are the kinetic and potential energies, respectively, of the system. The kinetic energy can be found from

$$T(t) = \frac{1}{2} m_{11} \dot{q}_1^2(t) \tag{7}$$

and the potential energy can be found from

$$V(t) = \frac{1}{2} k_{11} q_1^2(t), \tag{8}$$

where m_{11} is the generalized mass and k_{11} is the generalized stiffness of the system. Using (7) and (8), equation (6) becomes:

$$m_{11}\ddot{q}_1(t) + k_{11} q_1(t) = Q(t). \tag{9}$$

The generalized mass of the cylinder can be found from

$$m_{11} = a' \int_0^{2\pi} \int_0^L m(x, \alpha) \Phi_1^2(x, \alpha)\, dx\, d\alpha, \tag{10}$$

where $m(x, \theta)$ is the surface density of the cylinder. The generalized stiffness of the cylinder cannot be calculated as easily, but it can be approximated by

$$k_{11} \approx \omega_n^2 m_{11}, \tag{11}$$

where ω_n is the natural frequency found from equation (1).

When the piston is in sliding contact with the cylinder liner, the mass of the piston will modify the equivalent mass of the system. This effect can be included by calculating the generalized mass of the piston a point at a distance x_1 from the top of the cylinder liner. (Note: This approach assumes that the piston remains in contact with the cylinder liner after impact. The consequences

of this assumption will be discussed later in this paper.) The generalized mass of the piston M_p is

$$M_p = M\Phi_1^2(x_1, 0), \tag{12}$$

where M is the mass of the piston. M also includes the mass of the piston pin and the mass of that portion of the connecting rod assumed to be lumped at the piston.

The distance x_1 corresponds to the piston pin location and is found from the kinematics of the slider crank mechanism

$$x_1(t) = R + R_1\cos\theta - R_2[1 - (R_1/R_2)^2\sin^2\theta]^{1/2}, \tag{13}$$

where R is the distance from the crankshaft axis to the top of the cylinder liner, R_1 is the radius of the crankshaft, R_2 is the length of the connecting rod, and $\theta = \omega t$ is the angle of rotation of the crankshaft rotating with angular velocity ω; $\theta = 0$ is at the bottom-dead-center position of the piston.

The horizontal component of the force at the piston pin helps to hold the piston in contact with the liner after impact has occurred. Because this force is a time-varying one, it will excite the cylinder liner. Assuming that this force is applied at a point at a distance x_1 from the top of the cylinder liner, the generalized force is

$$Q(t) = F(t)\Phi_1(x_1, 0), \tag{14}$$

where x_1 is given by equation (13) and where $F(t)$ is the horizontal component of the force applied to the piston at the piston pin. This force can be found from [5]:

$$F(t) = \frac{R_1}{R_2}\left\{AP(\theta)\sin\theta - M\omega^2\left[\frac{R_1}{2}\sin 2\theta + \frac{R_1^2}{R_2}\sin 3\theta\right]\right\}, \tag{15}$$

where A is the area of the top surface of the piston and $P(\theta)$ is the cylinde pressure.

It can be seen from Fig. 3d that the cylinder liner vibration is underdamped, but it is difficult to calculate the damping in the system. Several damping mechanisms occur during piston impact. These include: structural damping of the cylinder liner and piston, damping due to oil-film cushioning and ring-groove friction [9], and damping due to the radiation of sound from the external surfaces of the cylinder liner. When such complex damping mechanisms occur in a system, it is common to estimate an equivalent viscous damping ratio from experimental data. Defining the equivalent damping ratio ζ, the generalized damping force is $2\zeta\omega_n(M_{11} + M_p)\dot{q}_1(t)$.

Using equations (9) and (11), as well as the above mentioned results for equivalent viscous damping, an equation representing an equivalent single-

degree-of-freedom system describing the vibration of the cylinder liner after impact is

$$\ddot{q}_1(t)+2\zeta\omega_n\dot{q}_1(t)+\left[\frac{\omega_n^2}{1+M_p/m_{11}}\right]q_1(t)=\frac{Q(t)}{m_{11}+M_p}. \tag{16}$$

This model is represented schematically in Fig. 6. Fig. 6a shows the model while the piston undergoes free-travel just prior to impact, while Fig. 6b represents the model after impact. During piston free-travel, equation (16) with $Q(t)$

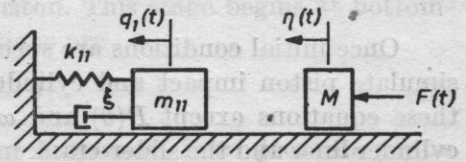

a)

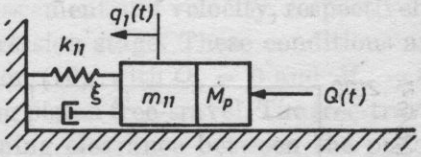

b)

Fig. 6. Models for piston impact and cylinder liner vibration
a – model during piston free-travel, b – model after impact

and M_p set equal to zero represents the motion of the cylinder liner. The motion of the piston during free-travel is governed by

$$F(t)=M\ddot{\eta}, \tag{17}$$

where $\eta(t)$ is the displacement of the piston; $\eta=0$ corresponds to the piston in contact with the non-impact side of the cylinder liner.

Some comments are in order concerning the shortcomings of the model represented by equations (16) and (17). A detailed model of damping has intentionally been avoided by the use of an equivalent viscous damping ratio determined from experimental data. The use of an experimentally determined damping ratio facilitates the description of the model, but provides very little insight into the actual damping mechanisms responsible for dissipation of the mechanical energy of the cylinder liner. This is a very challenging topic of research which was beyond the scope of the present study.

Equation (17) assumes that the piston motion during free-travel is pure translation. This is a highly ideal situation, and results in a very simple formula-

tion for the piston momentum just before impact. In practice, however, there exist unbalanced moments, due to friction and the fact that the piston pin does not usually coincide with the center-of-gravity of the piston, which impart angular momentum to the piston. These effects alter the piston-impact process by producing more than a single impact that results from equation (17). An example of a model that includes rotation is given in [7].

4. Initial conditions

Once initial conditions are specified, equations (16) and (17) can be used to simulate piston impact and cylinder liner vibration. All of the parameters in these equations except $P(\theta)$ and ω can be found from the dimensions of the cylinder liner and the slider-crank mechanism. $P(\theta)$ and ω describe the operating conditions of the engine and must be specified before simulation can take place. This information is usually known by engine designers from theoretical models or prototype engines. For this study the cylinder pressure was measured at rated horsepower and speed ($\omega = 220$ s^{-1},) with a piezoelectric pressure transducer mounted in the cylinder head above one of the cylinders. Fig. 7a shows the measured cylinder pressure (as a function of crankshaft angle), and

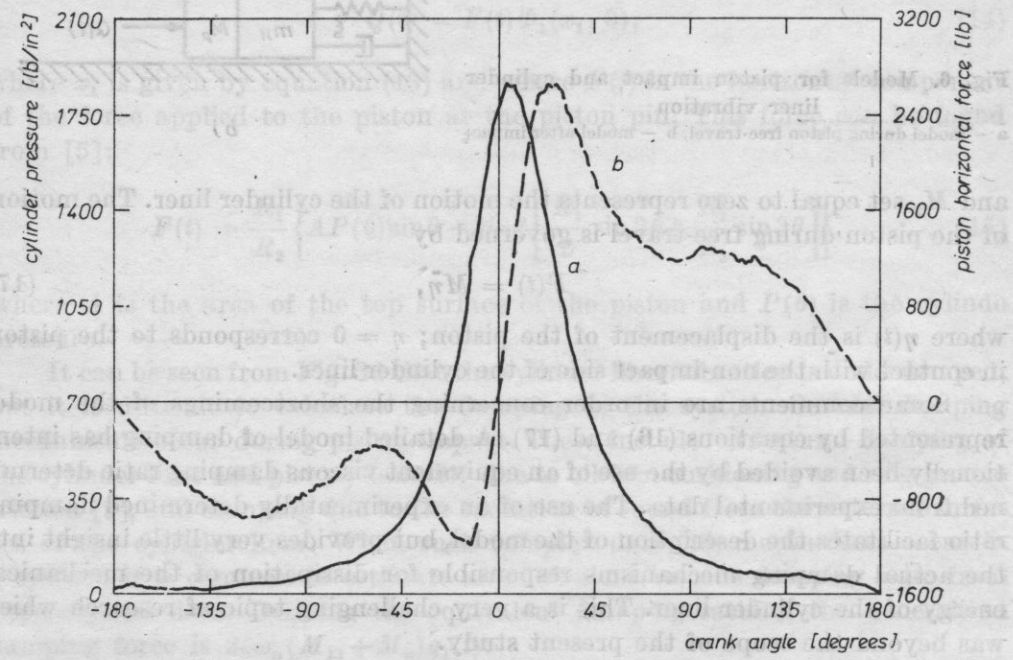

Fig. 7. a — cylinder pressure at rated horsepower as a function of crankshaft angle, b — horizontal component as piston force computed from Fig. 7a using equation (15)

Fig. 7b shows the horizontal component of the piston force computed from the data in Fig. 7a with the aid of equation (15).

The simulation is broken into three stages: the compression stage, in which the piston is in sliding contact with the nonimpact side of the cylinder liner; the free-travel stage, in which the piston traverses the cylinder bore; and the expansion stage, in which the piston is in sliding contact with the impact side of the cylinder liner. These stages are discussed below:

1. Compression stage ($0 \leqslant t \leqslant t_1$): During this stage equation (16) describes the behavior of the cylinder liner and the piston. This stage begins at bottom-dead-center ($\theta, t = 0$), and the initial conditions are

$$q(0) = \dot{q}(0) = 0, \tag{18}$$

i.e., it is assumed that no residual vibration is present from previous piston impacts. This stage terminates when $\theta = \pi$; at this point define $t = t_1$.

2. Free-travel stage ($t_1 < t \leqslant t_2$): During this stage equation (17) governs the piston motion, and the initial conditions are

$$\eta(t_1) = q_1(t_1), \quad \dot{\eta}(t_1) = \dot{q}_1(t_1), \tag{19}$$

where $q_1(t_1)$ and $\dot{q}_1(t_1)$ are the generalized displacement and velocity, respectively, of the cylinder liner at the end of the compression stage. These conditions are also used as initial conditions to solve equation (16), with $Q_p = 0$ and $M_p = 0$, to find the vibration of the cylinder liner during piston free-travel. The free-travel stage ends when $\eta = \delta$, where δ is the running clearance between the piston and the cylinder liner; at this point define $t = t_2$.

3. Expansion stage ($t_2 < t \leqslant t_3$): During this stage impact takes place and the piston is once more in sliding contact with the cylinder liner. Equation (16) governs the vibration of the cylinder liner. The initial displacement of the cylinder liner is $q_1(t_2^+) = q_1(t_2)$, but the initial condition of the generalized velocity must be determined from conservation of momentum. Just before impact the momentum of the piston is $M\dot{\eta}(t_2)$, and the generalized momentum of the liner is $M_{11}\dot{q}_1(t_2)$. The momentum of the piston/cylinder liner just after impact is $(M_p + m_{11})\dot{q}(t_2^+)$, and the initial generalized velocity for this stage is, therefore:

$$\dot{q}_1(t_2^+) = \frac{M\dot{\eta}(t_2) + m_{11}\dot{q}_1(t_2)}{M + m_{11}}. \tag{20}$$

Equation (20) assumes that the piston impact is inelastic (i.e., no piston rebound). This same assumption was made by FIELDING [7] in his work. Other experimental results indicate that rebound is very small [12] or nonexistent [11]. A careful study of the liner vibration (Fig. 3) with an expanded time scale did not reveal any evidence of multiple impacts. If rebound is found to occur, then equation (20) may be modified by including a coefficient of restitution [12].

5. Results and discussion

Using the data in Fig. 7a, along with the dimensions of the diesel engine used in this study [5], a simulation of the mathematical model was made using a digital computer. Fig. 8a shows the results of the computer simulation (solid line) and the measured cylinder liner acceleration time-history (dashed line) for the diesel engine operating at rated horsepower and speed.

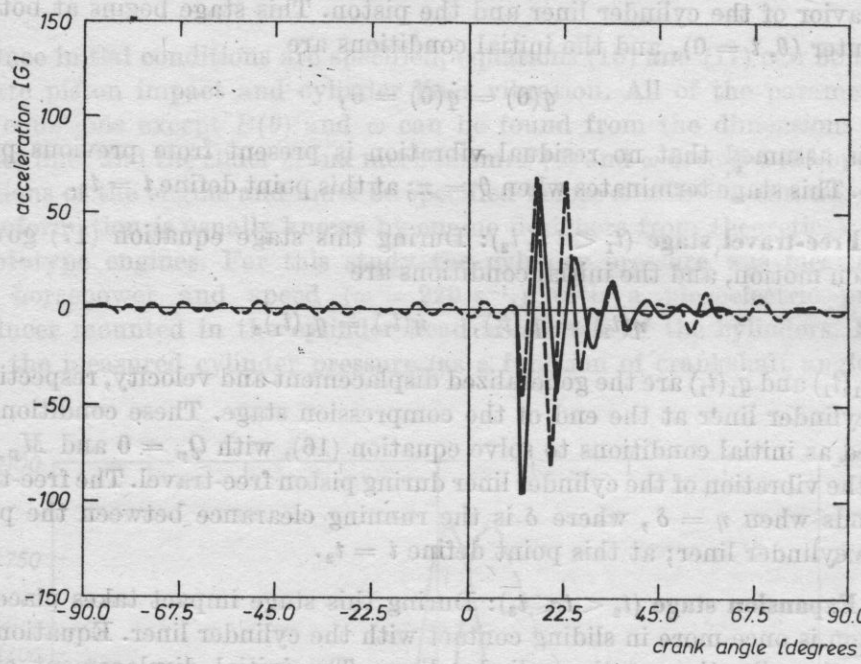

Fig. 8a. Measured (dashed line) and predicted (solid line) cylinder liner acceleration time-histories

The experimental data in Fig. 8a is the same data in Fig. 3a, but a low-pass filter (4000 Hz break frequency) was used to remove the high-frequency vibration that corrupted the original acceleration signal. Note, also, that the accelerations in Fig. 3 are inverted.

The actual cylinder liner and piston running clearance was not precisely known, but the manufacturer believed that it was in the range of 0.13 to 0.20 mm. A clearance of 0.18 mm accurately predicts the point of impact (approximately 12° after TDC) (see Fig. 8a). The damping ratio ζ used in the computer simulation was 0.13. This value of ζ was selected because it made the settling times of the experimental and computer simulation data approximately equal. The high value of damping cannot be accounted for solely by structural damping mecha-

nisms; other damping mechanisms, such as ring-groove friction and oil-film cushioning, are probably more important [11].

The simulation data in Fig. 8a show that cylinder liner vibration is negligible prior to piston impact, and that the vibration after impact is approximately zero for crankshaft angles exceeding 90°. For this example at least, the simulation could be simplified by omitting the compression stage portion of the mathematical model.

From Fig. 8a it can be seen that there is a difference in the overall form of the two acceleration time-histories. The results of the computer simulation show a very large acceleration immediately following impact; this acceleration decays exponentially, as expected for a single-degree-of-freedom system. In comparison, the initial measured acceleration is not nearly so large, but the acceleration during the second cycle of oscillation is very large. This behavior is perhaps due to oil-film cushioning and/or the presence of higher-order vibration modes.

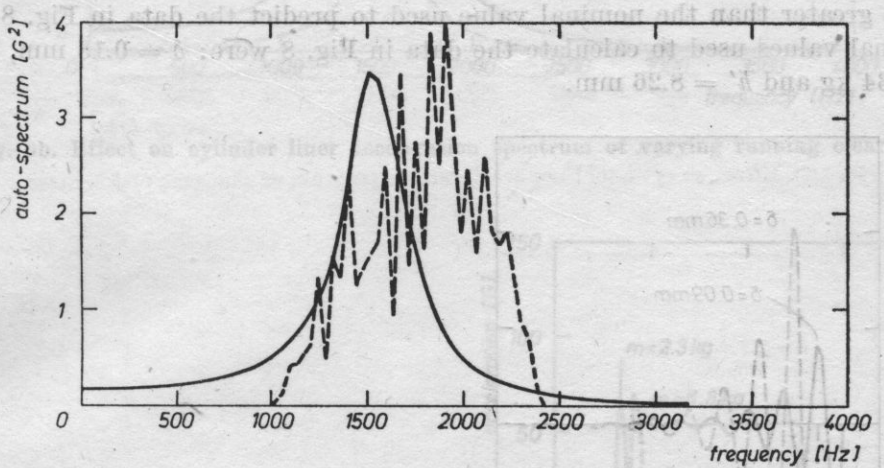

Fig. 8b. Measured (dashed line) and predicted (solid line) cylinder liner acceleration spectra (computed from Fig. 8a)

Fig. 8b shows a comparison between the acceleration spectra of the two signals in Fig. 8a. The frequency resolution of these data is 17.5 Hz, corresponding to the reciprocal of the period of one complete engine cycle (720° of crankshaft rotation). While these spectra agree in form, there are some discrepancies in magnitude and frequency. In Fig. 8b it can be seen that the spectrum of the experimental acceleration time-history has a considerable amount of random error superimposed upon the true spectrum. This random error could be reduced if more data had been used to compute a smooth spectrum by using ensemble-averaging methods.

6. Parameter study

The importance of the mathematical simulation described in this paper lies in its ability to assess the effect of design changes involving critical parameters such as running clearance and piston mass. The results in Fig. 8 show that the mathematical model is not sophisticated enough to accurately predict absolute values of cylinder liner vibration. However, the model does provide an estimate of the general trends in the experimental data. From the standpoint of engineering design, the model may be used to evaluate the effect of relative changes in design parameters. However, one must be careful not to vary the design parameters over a range that violates the assumptions used in formulating the mathematical model. For example, in evaluating the effect of cylinder liner thickness, one would not want to violate the condition $h' \ll a'$ which is an assumption used in the derivation of equation (1).

In this paper only three parameters — running clearance, piston mass, and cylinder liner thickness — are varied; a more complete parameter study is given in [5]. Each parameter is varied twice, one value less than and the other value greater than the nominal value used to predict the data in Fig. 8. The nominal values used to calculate the data in Fig. 8 were: $\delta = 0.18$ mm, $M = 5.34$ kg and $h' = 8.26$ mm.

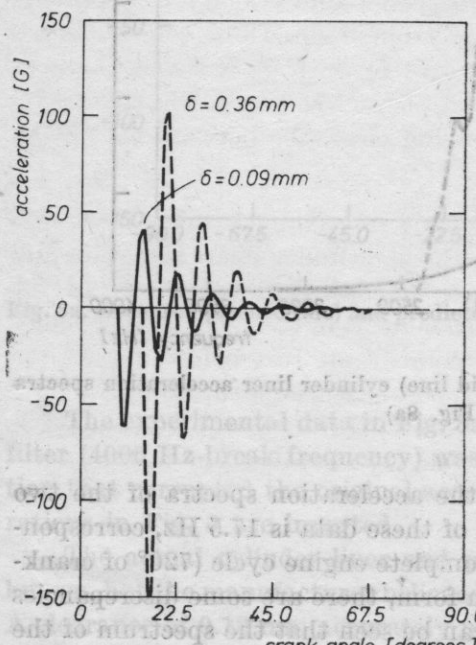

Fig. 9a. Effect on cylinder liner vibration time-history of varying running clearance

Fig. 9 shows the effect on cylinder liner vibration of varying the piston/cylinder liner running clearance δ. Fig. 9a compares the acceleration time-histories for δ equal to 0.090 mm and 0.36 mm. With the larger running clearance, piston

impact is delayed approximately 5°, and the peak acceleration is increased about 2 1/2 times. Fig. 9b shows the accelaration spectra computed from the time-histories in Fig. 9a. Fig. 9b shows that, near 1500 Hz, increasing the running clearance

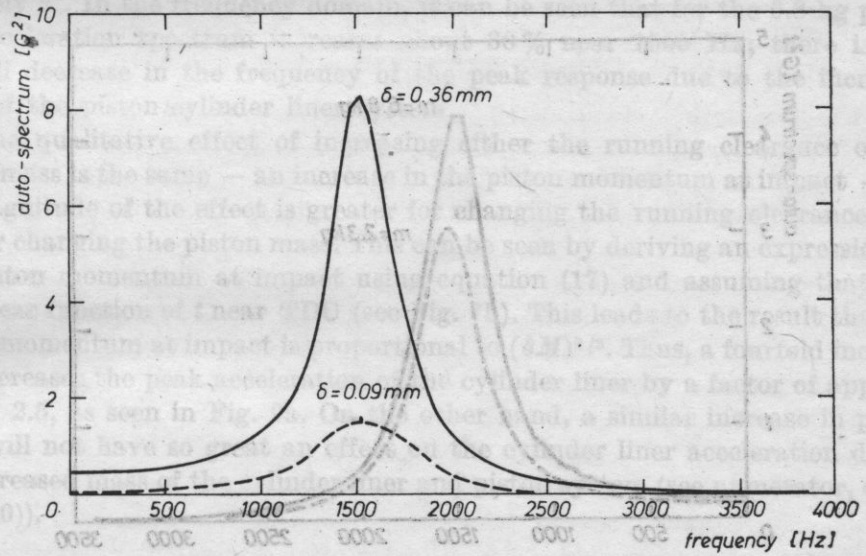

Fig. 9b. Effect on cylinder liner acceleration spectrum of varying running clearance

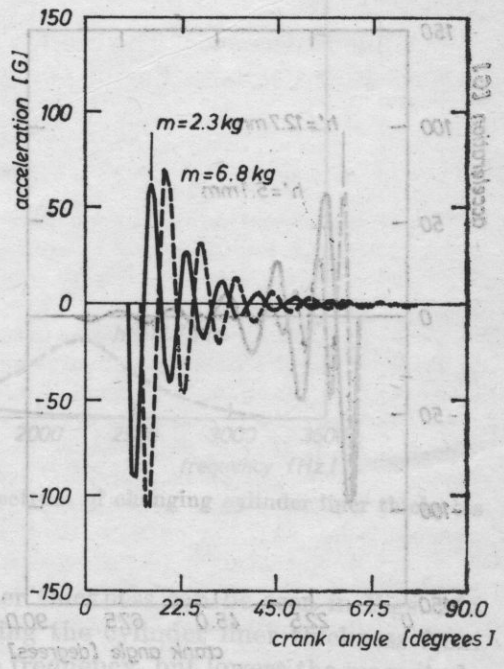

Fig. 10a. Effect on cylinder liner vibration of changing piston mass

has an effect more pronounced than is expected from the data in Fig. 9a. It can be seen from Fig. 9b that the peak response is increased by a factor of six due to a fourfold increase in δ.

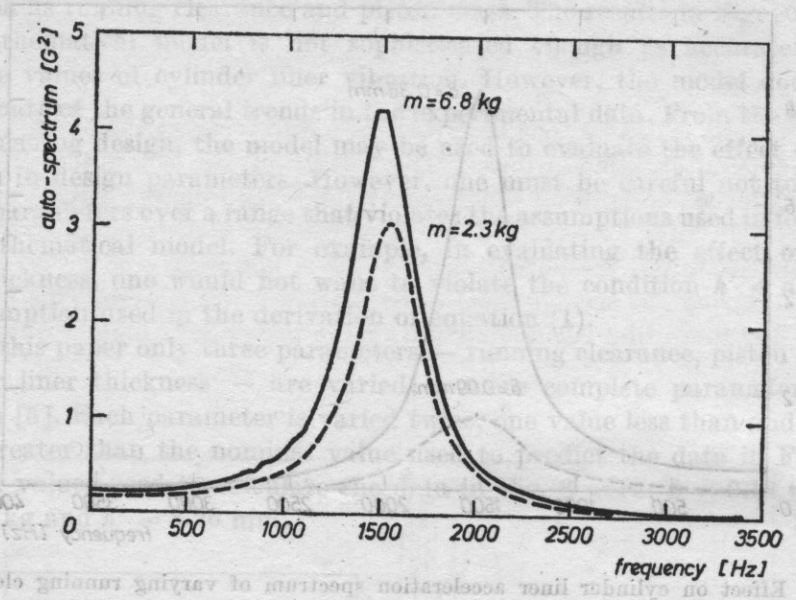

Fig. 10b. Effect on cylinder liner acceleration spectrum of changing piston mass

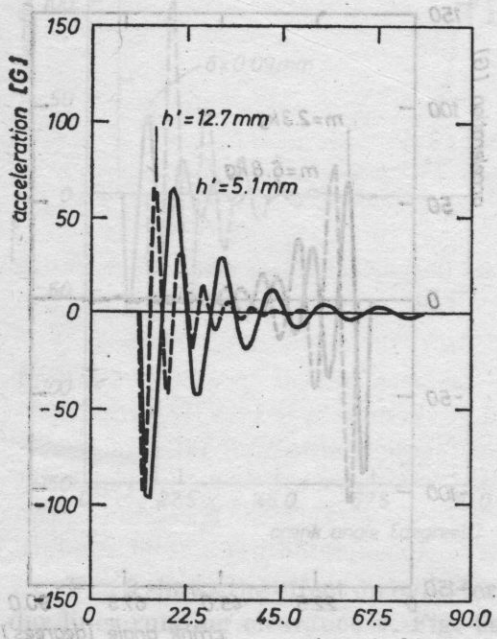

Fig. 11a. Effect on cylinder liner vibration of changing cylinder liner thickness

The effect of changes in piston mass can be seen in Figs. 10a and 10b. In the time domain, Fig. 10a, increasing the piston mass from 2.3 kg to 6.8 kg has only a small effect on the peak acceleration; the impact is delayed approximately 5°. In the frequency domain, it can be seen that for the 6.8 kg piston the acceleration spectrum increases about 30 % near 1500 Hz; there is also a small decrease in the frequency of the peak response due to the increased mass of the piston/cylinder liner system.

The qualitative effect of increasing either the running clearance or the piston mass is the same — an increase in the piston momentum at impact — but the magnitude of the effect is greater for changing the running clearance than it is for changing the piston mass. This can be seen by deriving an expression for the piston momentum at impact using equation (17) and assuming that $F(t)$ is a linear function of t near TDC (see Fig. 7b). This leads to the result that the piston momentum at impact is proportional to $(\delta M)^{2/3}$. Thus, a fourfold increase in δ increases the peak acceleration of the cylinder liner by a factor of approximately 2.5, as seen in Fig. 9a. On the other hand, a similar increase in piston mass will not have so great an effect on the cylinder liner acceleration due to the increased mass of the cylinder liner and piston system (see numerator, equation (20)).

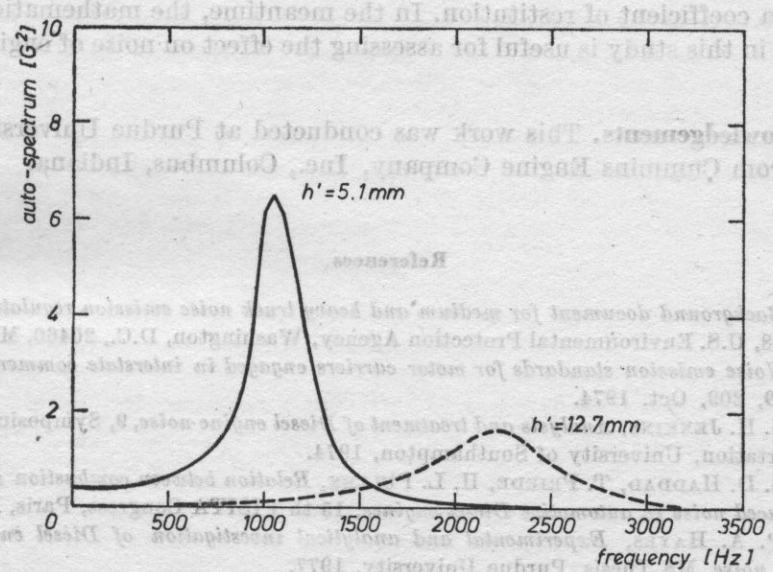

Fig. 11b. Effect on cylinder liner acceleration spectrum of changing cylinder liner thickness

The effect of altering the cylinder liner thickness can be seen in Figs. 11a and 11b. These figures show that increasing the cylinder liner thickness from 5.1 to 12.7 mm increases the peak-response frequency, but lowers the magnitude

of the peak response, Fig. 11b. Both of these effects can be explained by noting that increasing the cylinder liner thickness increases the stiffness and the natural frequency of the cylinder liner, equation (1).

7. Summary and conclusions

A simple mathematical model has been developed to study piston impact and cylinder liner vibration in internal combustion engines. The results of this model agree reasonably well with experimental data, although the model uses several simplifying assumptions. The cylinder liner was modeled as a thin cylindrical shell with fixed-free boundary conditions; only the fundamental mode of vibration of the shell was considered. The experimental data seem to support the use of a single-mode cylinder liner model, at least in the 500-3000 Hz frequency range where piston impact noise is important. During free-travel, the piston was assumed to move in pure translation only. Other piston models (e.g., [7]) include rotational effects; but in view of the results in this study perhaps rotation is of secondary importance.

The model could be refined when more information on piston impact is available. For example, a study of energy dissipation and momentum transfer mechanisms at impact would yield estimates of an equivalent viscous damping ratio and a coefficient of restitution. In the meantime, the mathematical model developed in this study is useful for assessing the effect on noise of engine design changes.

Acknowledgements. This work was conducted at Purdue University under support from Cummins Engine Company, Inc., Columbus, Indiana.

References

[1] *Background document for medium and heavy truck noise emission regulations*, EPA 550/9-76-008, U.S. Environmental Protection Agency, Washington, D.C., 20460, March, 1976

[2] *Noise emission standards for motor carriers engaged in interstate commerce*, Federal Register, **39**, 209, Oct. 1974.

[3] S. H. Jenkins, *Analysis and treatment of Diesel engine noise*, 9, Symposium on Noise in Transportation, University of Southampton, 1974.

[4] S. D. Haddad, T. Priede, H. L. Pullen, *Relation between combustion and mechanically induced noise in automotive Diesel engines*, 15 th FISITA Congress, Paris, 1974.

[5] P. A. Hayes, *Experimental and analytical investigation of Diesel engine piston impact and noise*, MS Thesis, Purdue University, 1977.

[6] P. A. Hayes, A. F. Seybert, J. F. Hamilton, *A coherence model for piston-impact generated noise*, SAE Engine Noise Conference, P-80, 125-132, 1980.

[7] B. J. Fielding, *Identification of mechanical sources of noise in a Diesel engine*, Ph. D. Thesis, University of Manchester, England, 1968.

[8] B. J. Fielding, J. Skorecki, *Identification of mechanical sources of noise in a Diesel engine: sound originating from piston slap*, Proceedings, Institution of Mechanical Engineers, **184**, 857-873 (1969-70).

[9] Y. FUJIMOTO, et al., *Experimental studies on piston slap in reciprocating machinery* (in Japanese), preprint of JSME, March 1976.

[10] T. SUZUKI, et al., *Studies on piston slap in reciprocating machinery* (in Japanese), preprint of JSME, March 1976.

[11] Y. FUJIMOTO, T. SUZUKI, Y. OCHIAI, *On piston slap in reciprocating machinery*, Vibration in Rotating Machinery, Institution of Mechanical Engineers, c215/76 (1976).

[12] S. D. HADDAD, P. W. FORTESCUE, *Simulating piston slap by an analog computer*, Journal of Sound and Vibration, **52**, 1, 79-93 (1977).

[13] S. D. HADDAD, *Origins of noise and vibration in vee form Diesel engines with emphasis on piston slap*, Ph. D. Thesis, University of Southampton, 1974.

[14] H. KRAUS, *Thin elastic shells*, 132, John Wiley and Sons, Inc., 1967.

[15] L. MEIROVITCH, *Elements of vibration analysis*, section 7.4, McGraw Hill, 1975.

Received on January 18, 1980